Verifying continuous variable entanglement of intense light pulses

Oliver Glöckl,* Ulrik L. Andersen, and Gerd Leuchs
Institut für Optik, Information und Photonik, Max–Planck Forschungsgruppe, Universität Erlangen–Nürnberg, Günther–Scharowsky–Straße 1 / Bau 24, 91058 Erlangen, Germany
(Dated: February 9, 2008)

Three different methods have been discussed to verify continuous variable entanglement of intense light beams. We demonstrate all three methods using the same set–up to facilitate the comparison. The non–linearity used to generate entanglement is the Kerr–effect in optical fibres. Due to the brightness of the entangled pulses, standard homodyne detection is not an appropriate tool for the verification. However, we show that by using large asymmetric interferometers on each beam individually, two non-commuting variables can be accessed and the presence of entanglement verified via joint measurements on the two beams. Alternatively, we witness entanglement by combining the two beams on a beam splitter that yields certain linear combinations of quadrature amplitudes which suffice to prove the presence of entanglement.

PACS numbers: 03.67.Mn, 42.50.Dv, 42.50.Lc

I. INTRODUCTION

About 70 years after Einstein described it as "spooky interactions at a distance" [1], the phenomenon of entanglement is one of the most intriguing and useful properties of quantum mechanics. In the very early days of entanglement its philosophical mindboogling implications dominated the discussion; later it served as an experimental testbed for the foundations of quantum mechanics and recently the usage of entanglement has facilitated a revolution in information science holding the promise to efficiently solve hard computational problems and guranteeing secure communication [2]. More specifically, entanglement is the key physical resource enabling the successful execution of many quantum information protocols, prominent examples being quantum teleportation [3] and quantum dense coding [4]. These protocols were initially proposed for discrete variables, but recently protocols utilizing continuous quantum variables, such as the quadrature amplitudes of the electromagnetic field, have emerged as an interesting alternative [5]. Therefore over the last few years there has been a desire to develop efficient and compact sources of entanglement where quadrature variables of the light state are quantum mechanically correlated which is normally coined quadrature entanglement.

To date many convincing experimental realisations of quadrature entanglement have been conducted based on different nonlinear effects in different media such as the second order nonlinearity in optical parametric oscillators either utilizing a single nondegenerate OPO (in polarization [6, 7, 8], frequency [9, 10] or direction [11]) or two degenerate OPOs [12, 13, 14], and the third order nonlinearity in atoms [15] or fibers [16]. After the production of entanglement it is crucial to have some experimental characterisation methods at hand by which one can determine whether the system contains truely quantum mechanical correlations.

In all the above mentioned experiments, Gaussian states were assumed to be produced. In this case complete information about the system, including the amount of entanglement, is contained in the covariance matrix. However, instead of measuring all entries of the covariance matrix (which is quite demanding, experimentally) the variance of certain linear combinations of the quadrature variables suffice to witness the presence of entanglement [17, 18, 19]. Such a criterion for entanglement was used in all the experiments listed above. In most of the experiments homodyne detection on each subsystem (relying on two strong local oscillators) followed by classical communication between them were used to generate the appropriate linear combinations and subsequently witness the presence of entanglement. Such an approach was indeed valid in these experiments since the entangled beams under investigations either did not have an optical carrier or one that was negligible small compared to that of that of the local oscillator. However, by exploiting the Kerr effect in fibers to generate squeezing and subsequently entanglement, pulses containing on the order of 10^8 photons or more per pulse are needed to compensate for the almost vanishing small Kerr nonlinearity in standard glass fibers. In turn this practically excludes the usage of homodyne detection techniques since this will require local oscillator pulses containing more than 10^{10} photons and hence detectors capable of handling high power pulses and simultaneously measuring at the quantum noise limit, a technology which is not, at present, technically feasible.

In this paper we present a careful verification of the presence of entanglement between intense pulses by constructing the proper linear combination of noncommuting quadrature variables by means of three different measurement strategies. In the first method we prove entanglement by measuring locally the amplitude and phase quadratures of the two beam and compare the outcomes using classical communication. Here the conjugate

*Electronic address: gloeckl@kerr.physik.uni-erlangen.de

quadratures of the respective beams are measured using an interferometric method [20]. As an alternative, we verify entanglement between two beams by interfering them on a beam splitter and then by controlling their relative phase shift, we are able to measure the correlations of the conjugate quadratures either separately by comparing the two outputs from the beam splitter or jointly by monitoring a single output. The latter method was applied in ref. [16] to verify the presence of entanglement. Here we elaborate on the work of ref. [16] by conducting a more careful analysis of the different methods by which proper linear combinations of quadrature operators can be constructed to witness the presence of entanglement.

The paper is structured as follows. In section II, we review how continuous variable entanglement is generated by a linear combination of two squeezed beams on a beam splitter and how the presence of entanglement can be detected using a criterion based on quantities that can be accessed easily in experiments. In section III, a description of the experimental setup is outlined. Section IV, which constitutes the main part of this paper, is devoted to a careful description of the three different experimental approaches used to extract the linear combination of quadrature variables that proves the presence of entanglement. In section V we conclude the work.

II. ENTANGLEMENT PRODUCTION AND VERIFICATION

For the theoretical description of squeezing and entanglement with intense light beams, we use a linearized approach in a rotating frame. The field mode $\hat{a}$ is described by $\hat{a} = \alpha\hat{\mathbb{1}} + \delta\hat{a}$. α describes the steady state amplitude of the bright carrier with the frequency ω while the quantum character arising from sideband pairs is combined in the fluctuating part $\delta\hat{a}$. For Gaussian states $\delta\hat{a}$ can be written as a superposition of the amplitude quadrature $\delta\hat{\mathcal{X}}$ and the phase quadrature $\delta\hat{\mathcal{Y}}$: $\delta\hat{a} = \frac{1}{2}(\delta\hat{\mathcal{X}} + i\delta\hat{\mathcal{Y}})$. Throughout this paper, we refer to the amplitude quadrature as the direction along the classical amplitude excitation while the phase quadrature is the noise component perpendicular to the amplitude, i. e. we use a coordinate system denoted by $\delta\hat{X}$ and $\delta\hat{Y}$ that is rotated by the angle φ (corresponding to the classical phase of the mode). We are furthermore interested in the fluctuations around the mean values $\mathcal{X}/2$ and $\mathcal{Y}/2$, hence the new coordinate system $\delta\hat{X}$ and $\delta\hat{Y}$ is displaced by $\mathcal{X}/2$ and $\mathcal{Y}/2$. For a visualization of the notation, see the inset at the bottom of fig. 1.

To characterize the quantum state of a light mode, the spectral variances of the amplitude and the phase quadrature components $\delta\hat{X}$ and $\delta\hat{Y}$ at a certain sideband frequency Ω are determined by spectral analysis of photocurrents. Measurements of the amplitude quadrature is easily done in direct photo detection. The amplitude quadrature is then obtained from a photon number measurement under a linear approximation assumption:

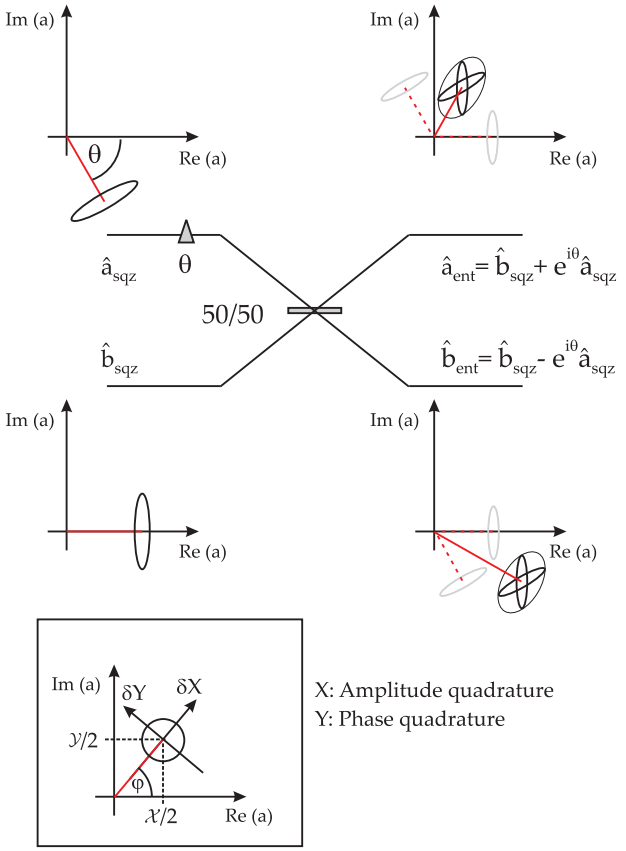

FIG. 1: Schematic representation of entanglement generation in a phase space diagram. Two bright amplitude squeezed beams interfere with relative phase θ at a 50/50 beamsplitter. Note that the plotted situation corresponds to non ideal entanglement generation where $\theta \neq \pi/2$, the resulting uncertainty areas are elliptical and the uncertainty in amplitude and phase is different for the two modes. Throughout this paper, the amplitude quadrature $\hat{X}$ is defined to point along the direction of the classical excitation, the phase quadrature $\hat{Y}$ is perpendicular (see inset).

$\hat{n}_a(t) = \hat{a}^\dagger\hat{a} = |\alpha|^2\hat{\mathbb{1}} + |\alpha|\delta\hat{X}_a(t)$, where $\delta\hat{X}_a$ denotes the fluctuations of the amplitude quadrature along the classical excitation. The detection of the conjugate variable, the phase quadrature $\delta\hat{Y}$, is more involved, as this requires the introduction of a relative phase shift of the bright carrier mode α with respect to the sideband modes $\delta\hat{a}$. A detailed analysis of a measurement technique to obtain information about the phase quadrature component of a light beam as well as correlation measurements of the phase quadrature via a joint measurement on a pair of beams is the subject of section IV.

Quadrature entanglement is achieved by linear interference of two intense amplitude squeezed modes $\hat{a}_{sqz}$ and $\hat{b}_{sqz}$ on a beam splitter[12, 21, 22]. A phase space representation of this process is shown in figure 1. We assume that both squeezed input beams have the same classical amplitudes $\alpha_{sqz} = \beta_{sqz} = \alpha$ as well as the same variances for the squeezed and the antisqueezed quadrature

respectively: $V(\delta\hat{X}_{\rm a,sqz}) = V(\delta\hat{X}_{\rm b,sqz}) \equiv V(\delta\hat{X}_{\rm sqz})$ and $V(\delta\hat{Y}_{\rm a,sqz}) = V(\delta\hat{Y}_{\rm b,sqz}) \equiv V(\delta\hat{Y}_{\rm sqz})$. Depending on the relative interference phase θ, entangled output states $\hat{a}_{\rm ent}$ and $\hat{b}_{\rm ent}$ are generated, with the classical amplitudes

$$\alpha_{\rm ent} = \alpha\sqrt{1+\cos\theta} \quad (1)$$

$$\beta_{\rm ent} = \alpha\sqrt{1-\cos\theta}. \quad (2)$$

The quadrature components of the entangled output modes $\delta\hat{X}_{\rm a,ent}$, $\delta\hat{Y}_{\rm a,ent}$, $\delta\hat{X}_{\rm b,ent}$ and $\delta\hat{Y}_{\rm b,ent}$ are given in terms of the input squeezed beams and the interference phase θ

$$\delta\hat{X}_{\rm a,ent} = \frac{1}{2}\frac{1}{\sqrt{1+\cos\theta}}[(1+\cos\theta)\delta\hat{X}_{\rm a,sqz} + (1+\cos\theta)\delta\hat{X}_{\rm b,sqz} + \sin\theta\delta\hat{Y}_{\rm a,sqz} - \sin\theta\delta\hat{Y}_{\rm b,sqz}], \quad (3)$$

$$\delta\hat{Y}_{\rm a,ent} = \frac{1}{2}\frac{1}{\sqrt{1+\cos\theta}}[(1+\cos\theta)\delta\hat{Y}_{\rm a,sqz} + (1+\cos\theta)\delta\hat{Y}_{\rm b,sqz} - \sin\theta\delta\hat{X}_{\rm a,sqz} + \sin\theta\delta\hat{X}_{\rm b,sqz}], \quad (4)$$

$$\delta\hat{X}_{\rm b,ent} = \frac{1}{2}\frac{1}{\sqrt{1-\cos\theta}}[(1-\cos\theta)\delta\hat{X}_{\rm a,sqz} + (1-\cos\theta)\delta\hat{X}_{\rm b,sqz} - \sin\theta\delta\hat{Y}_{\rm a,sqz} + \sin\theta\delta\hat{Y}_{\rm b,sqz}], \quad (5)$$

$$\delta\hat{Y}_{\rm b,ent} = \frac{1}{2}\frac{1}{\sqrt{1-\cos\theta}}[(1-\cos\theta)\delta\hat{Y}_{\rm a,sqz} + (1-\cos\theta)\delta\hat{Y}_{\rm b,sqz} + \sin\theta\delta\hat{X}_{\rm a,sqz} - \sin\theta\delta\hat{X}_{\rm b,sqz}]. \quad (6)$$

Pairs of quadratures are strongly correlated, in particular, for $\theta = \pi/2$ where $(\delta\hat{X}_{\rm a,ent} + \delta\hat{X}_{\rm b,ent}) \to 0$ and $(\delta\hat{Y}_{\rm a,ent} - \delta\hat{Y}_{\rm b,ent}) \to 0$ for strongly squeezed input fields. For this particular choice of the interference phase the variances of the joint variables are

$$V(\delta\hat{X}_{\rm a,ent} + \delta\hat{X}_{\rm b,ent}) = 2V(\delta\hat{X}_{\rm sqz}), \quad (7)$$

$$V(\delta\hat{Y}_{\rm a,ent} - \delta\hat{Y}_{\rm b,ent}) = 2V(\delta\hat{X}_{\rm sqz}), \quad (8)$$

i. e. they only depend on the squeezing level. However, if the relative interference phase θ between the two amplitude squeezed states is different from $\pi/2$, the generated entanglement will not have the largest possible value [23]. In such a case the uncertainty areas in phase space become asymmetric as illustrated in figure 1, and as a result the correlations between quadratures of the two beams reduces.

To characterize entanglement, a well established approach is to consider the criterion derived by Duan et al. [18] and Simon [19]: Entanglement or equivalently non–separability is present in the system if [24]

$$V^{\pm}_{\rm sq}(\delta\hat{X}) + V^{\mp}_{\rm sq}(\delta\hat{Y}) < 2. \quad (9)$$

The correlations are expressed by the squeezing variances

$$V^{\pm}_{\rm sq}(\delta\hat{X}) = \frac{V(\delta\hat{X}_1 \pm g\delta\hat{X}_2)}{V(\delta\hat{X}_{1,\rm coh} + g\delta\hat{X}_{2,\rm coh})}, \quad (10)$$

$$V^{\mp}_{\rm sq}(\delta\hat{Y}) = \frac{V(\delta\hat{Y}_1 \mp g\delta\hat{Y}_2)}{V(\delta\hat{Y}_{1,\rm coh} + g\delta\hat{Y}_{2,\rm coh})}. \quad (11)$$

The variances are normalized to the shot noise level of coherent states, indicated by the subscripts "coh". Here, g is a variable gain that could be optimized to minimize the correlation signal. For the symmetric case described above, $g = 1$. Though in general only sufficient, the criterion of inequality (9) provides an experimentally easy measure to check whether or not a given state is entangled. Note that by application of local unitary squeezing operations, the sum criterion of equation (9) can be transformed into a product criterion [25, 26, 27]

$$V^{\pm}_{\rm sq}(\delta\hat{X}) \times V^{\mp}_{\rm sq}(\delta\hat{Y}) < 1. \quad (12)$$

The criterion in product form is more general than the criterion given by eqn. (9), as a larger class of entangled states can be witnessed (in particular for biased forms of entanglement). Although the product form is in general more appropriate to verify entanglement experimentally [13], in this paper we use the sum form as it will facilitate the comparison of the different entanglement measurement schemes to be presented. As will become clear in the following, one of the measurement strategies delivers directly the sum criterion with no access to the product.

The main purpose of this paper is to describe various methods by which a proper linear combination of non commuting quadrature operators can be constructed to yield the squeezing variances defined in eqns. (10) and (11). Having these variances at our disposal non–separability can subsequently be determined using the criterion (9).

III. EXPERIMENTAL GENERATION OF ENTANGLEMENT USING FIBER OPTICS

In this section, we present a setup to generate intense, pulsed, amplitude squeezed light using an asymmetric fiber Sagnac interferometer (see Fig. 2). Intense light pulses are split into a strong and a weak pulse at an asymmetric beam splitter. These pulses are coupled from different directions into an optical fiber. After counter propagating through the fiber, the pulses interfere again at the beam splitter. Squeezing is produced by exploiting the Kerr nonlinearity: the strong light pulses acquire an intensity dependent phase shift. Thus, the initially circular shaped uncertainty area in phase space is transformed into an ellipse. By interference with the weak pulse, the uncertainty ellipse is reoriented in phase space, resulting in directly detectable amplitude squeezing [28, 29].

In the experiment we use pulses with a duration of about 130 fs at a center wavelength of 1530 nm and at a repetition rate of 82 MHz. The pulses were produced by an optical parametric oscillator (Spectra physics,OPAL) pumped by a Ti:Sapphire Laser (Spectra Physics,Tsunami). These pulses are injected into the asymmetric fiber Sagnac interferometer (Fig. 2). This is operated simultaneously at two orthogonal polarizations to obtain two amplitude squeezed beams with equal optical power for the generation of entanglement. The

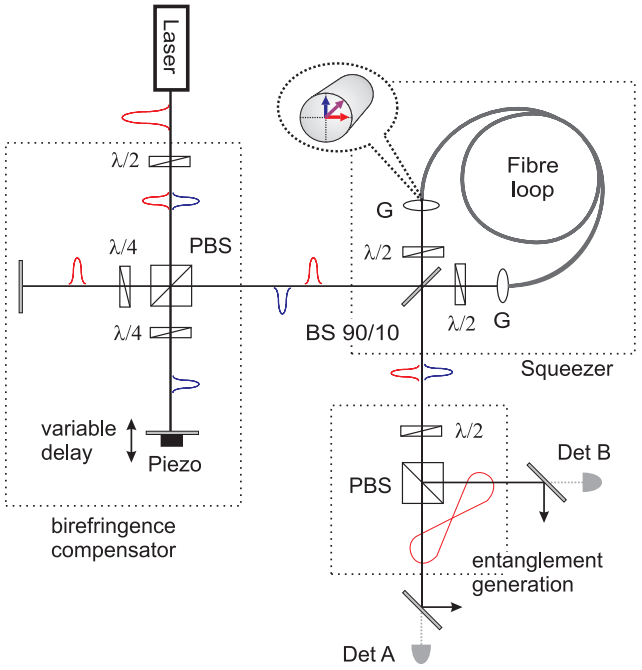

FIG. 2: Setup for entanglement generation. Two squeezed beams of orthogonal polarization are generated in an asymmetric fiber Sagnac interferometer and are brought to interference at a polarizing beam splitter (PBS) together with a $\lambda/2$–waveplate. To control the relative phase of the two pulses and to compensate their relative delay due to the birefringence of the fiber, a Michelson interferometer is placed in front of the Sagnac loop. G: Gradient index lens, Det A and B: DC–detectors for phase lock, BS: beam splitter.

Sagnac loop consists of 8 m polarization maintaining fiber (3M, FS–PM–7811) and an asymmetric 90/10 beam splitter. In a previous experiment [16], the generation of quadrature entanglement by the interference between the two amplitude squeezed pulses on a 50/50 beam splitter was reported. The two orthogonally polarized squeezed modes were divided at a polarizing beam splitter into two spatial modes. Before interference, the polarizations of both modes were matched and the relative delay of the two pulses due to the birefringence of the fiber was compensated.

In our experiment, the squeezed pulses emerging the Sagnac loop in orthogonal polarization modes are already overlapping, not only spatially but also temporally. This is achieved by inserting a birefringence compensator in front of the Sagnac loop. This device is basically a Michelson interferometer, that introduces different delays for the two polarizations. Similar techniques were used by Fiorentino et al. [30] to generate amplitude squeezing using a fiber in a Mach–Zehnder like configuration and by Heersink et al. [31] where polarization squeezing was demonstrated. In order to mix the two squeezed modes and hence to generate quadrature entanglement, a polarizing beam splitter together with a $\lambda/2$–plate is inserted after the fiber. This allows for the possibility to carefully align the splitting ratio of the entangling beam splitter. To sucessfully generate entanglement, not only the delay due to the birefringence must be compensated, but also the relative optical phase of the two pulses must be actively locked using a feedback control system to ensure maximum entanglement with the given resources. As noted above, this corresponds to $\theta = \pi/2$ and hence balanced intensities of the output beams. To create an error signal for the feed back control of the piezo mirror in the Michelson–interferometer, the difference of the optical power of the individual entangled beams must be recorded. This signal is accessed by detecting the fraction of light that is leaking through high reflecting mirrors ($R > 99.5\%$) using a pair of high–gain detectors (Det A and Det B, in figure 2). The advantage of using such a system is its high stability, the almost perfect spatial overlap of the two squeezed beams and minimized losses allowing for an interference contrast of 99.5%.

One specific feature of Kerr–squeezed states from optical fibers is the high degree of excess phase noise that is acquired during propagation through the fiber [32] due to guided acoustic wave Brillouin scattering (GAWBS) [33] and self phase modulation. The excess noise in the phase quadrature was more than 20dB above the shot noise limit as will be seen from the measurements presented below. For the generation of entanglement, this is not a problem in principle as the phase noise leads to classically correlated noise in the entangled output beams which cancels in the correlation measurements. However, the phase noise does play a role when the beam splitter for the entanglement generation is not well balanced, that is the splitting ratio is different from 50/50. In that case, phase correlations are degraded as the cancellation of the correlated noise is no longer perfect. In our experiment, the excess phase noise turned out to be a limiting factor for the entanglement generation. However, the negative effects on the correlation in the phase quadrature was minimized by adjusting the splitting ratio of the beam splitter properly.

IV. EXPERIMENTAL TECHNIQUES, MEASUREMENT METHODS AND RESULTS

In the following section, we present several experimental techniques which are capable of generating the linear combination of quadratures needed to witness entanglement. The schemes are all based on interferometric set–ups which do not require an external local oscillator and hence are applicable for intense, pulsed light. Each technique described below is accompanied by experimental results.

In all experiments, we evaluate the spectral variances of the detected light field at a certain side band frequency Ω. The detected signal is actually the result of a beating between the bright carrier component of the light field with a pair of quantum side bands separated symmetrically from the carrier by Ω. The spectral variance or the

noise power is obtained experimentally from the photo current of the detectors with a spectrum analyser (HP 8590). As detectors we used InGaAs photodiodes (Epitaxx ETX500). All measurements were performed at a center frequency of 20.5MHz or 17.5MHz, the resolution bandwidth was 300kHz and for averaging, a video bandwidth of 30Hz was chosen.

A. Phase measurements on intense light beams

The most intuitive way of constructing the linear combination of quadratures that can witness entanglement is to simultaneously measure the amplitude quadrature (phase quadrature) of the two beams and subsequently add (subtract) the outcomes. The amplitude quadrature of intense, pulsed light can be accessed rather easily in direct detection with a pair of balanced detectors. However, detection of the phase quadrature is more involved. This quadrature is normally accessed using a homodyne detector[34] where the signal beam interferes with a much stronger local oscillator. For intense signal beams, this gives rise to technical difficulties as the high intensities may saturate the detectors. Alternatively, phase measurements of bright beams can be achieved by reflecting the light off a detuned cavity. A frequency dependent phase shift is introduced due to multiple beam interference, and as a result the bright carrier is rotated with respect to the sidebands [35, 36]. This technique was used in some early quantum optical experiments using fibers [37, 38]. For ultra short light pulses however, the requirements for the dispersion properties of the resonator are quite demanding.

In this section, we present another approach to measure the fluctuations of the phase quadrature at a certain sideband frequency without the need of an external local oscillator or a cavity. The scheme is thus suitable for the intense, pulsed beams used in our experiment and correlations in the phase quadrature as well as in the amplitude quadrature could be verified directly by performing separate measurements on the entangled beam pair. Towards this goal we employed a Mach–Zehnder interferometer with an unbalanced arm length difference [20] (see Fig. 3a). In this interferometer, a phase shift between the carrier and the sidebands (which are separated from the carrier with the frequency Ω) is introduced due to free space propagation and two beam interference. This phase shift is achieved by splitting the input beam $\hat{a} = \alpha\hat{\mathbb{1}} + \delta\hat{a}$ into two parts and subsequently delaying one beam with respect to the other by a length ΔL. This delay is chosen such that a phase shift of π is acquired between the sideband modes under investigation with respect to the carrier, corresponding to $\Delta L = c/2f$ where $f = \Omega/2\pi$ is the measurement frequency. The beams interfere on a second beam splitter with the relative optical phase set to $\pi/2$, resulting in two equally bright output beams. Direct photodetection is performed in the two output ports of the interferometer, and by taking the

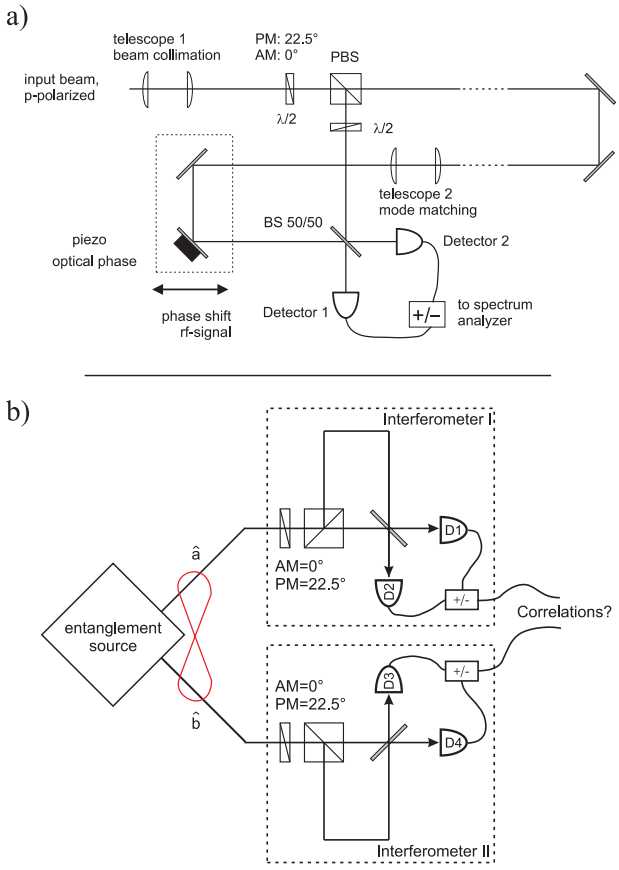

FIG. 3: a) Experimental setup of the phase-measuring interferometer. The orientation of the first $\lambda/2$-plate determines the type of measurement: amplitude measurement (AM) or phase measurement (PM). PBS, polarizing beam splitter; 50 50, beam splitter. b) Schematic of the setup to verify entanglement using two phase measuring interferometers.

difference of the photo currents, its spectral variance at the frequency Ω can be measured. The signal is proportional to the spectral variance of the phase quadrature of the input mode $\hat{a}$ at the side band frequency Ω [20]:

$$V(\delta\hat{n}_c - \delta\hat{n}_d) = \alpha^2 V(\delta\hat{Y}_a). \tag{13}$$

Using a pulsed laser system, as in our case, phase measurements can be performed only at certain frequencies, as possible delays where interference occurs are governed by the repetition frequency f_{rep} of the laser: $\Delta L = cn/f_{\mathrm{rep}}$ (n is an integer number). Possible measurement frequencies are then given by $f_m = f_{\mathrm{rep}}/2n$. With a repetition rate of 82 MHz, the arm length difference thus must be a multiple of 3.66 m, corresponding to the distance between two successive pulses. For a measurement at a frequency of 20.5 MHz an arm length difference of 7.32 m is required. A more detailed analysis of the phase measuring interferometer can be found in Ref. [20]. The set–up allows for easy switching between measurements of the phase quadrature and the amplitude quadrature. This is simply done by rotating the polarization of the input state. Since the first beam splitter of

the interferometer is a polarizing beam splitter, one can switch between the following two operation modes: (i) the intensity is distributed equally in both arms of the interferometer, and by interfering the beams at the second beam splitter phase measurements are performed (ii) all light propagates through one arm of the interferometer, the second beam splitter together with the detector pair comprises a balanced detector and amplitude measurements are performed.

To characterize entanglement, we have set up two such phase measuring interferometers in the output ports of the entanglement setup (see Fig. 3b). First, we have investigated the input squeezing that is used to generate entanglement. Using the interferometric setup in its amplitude measuring settings, we found squeezing levels of 2.5 ± 0.1dB (2.7 ± 0.1dB) for the p (s)–polarized beam. Then, entanglement was generated by interference of the squeezed beams. We have measured the amplitude quadratures as well as the phase quadratures of the two entangled modes $\hat{a}_{\rm ent}$ and $\hat{b}_{\rm ent}$ independently at different locations. The experimental results are summarized in figure 4. In (a) traces of amplitude noise measurements of the modes $\hat{a}_{\rm ent}$ and $\hat{b}_{\rm ent}$ are plotted. Traces 3 indicate the noise levels of the individual beams, i. e. $V(\delta\hat{X}_a)$ and $V(\delta\hat{X}_b)$. Clearly, both modes have the same noise level and exhibit a high degree of excess noise, corresponding to the noisy phase quadrature component of the input squeezed states. As discussed above, the high noise level is the result of the antisqueezing required by the Heisenberg uncertainty relation, but also due to additional thermal phase noise introduced by the fiber [33]. The noise level of the individual beams is more than 20dB above the quantum noise level. However, strong anti–correlations were observed as the variance of the sum signal of the amplitude quadratures $V(\delta\hat{X}_a + \delta\hat{X}_b)$ (trace 1) drops even below the respective shot noise level for the combined modes (trace 2) by 2.6dB. The squeezing variance to describe the amplitude correlation signal therefore is given by $V^+_{\rm sq}(\delta\hat{X}) = 0.55 \pm 0.02$ indicating strong non–classical correlations. On the other hand, the correlation signal, that is the difference signal of the amplitude quadratures $V(\delta\hat{X}_a - \delta\hat{X}_b)$ is 6dB above the noise level of the individual beams (see trace 4). Of these 6dB of noise, 3dB are due to the quantum correlations between the two modes whereas the other 3dB comes from the doubling in optical power. The errors indicated in this last and the following measurements were estimated from the standard deviation of 400 values obtained for the noise power with a spectrum analyzer at a resolution bandwidth of 300kHz and at a video bandwidth of 30Hz.

In part (b) of figure 4, the result of the correlations in the phase quadrature are plotted. Again, the individual beams exhibit a high degree of noise (traces 3), the noise level being of the same order as that of the amplitude quadrature. Strong non–classical correlations are observed for the phase quadrature, the variance of the difference signal $V(\delta\hat{Y}_a - \delta\hat{Y}_b)$ (trace 1) being 1.3dB below the quantum noise level (trace 2). The corresponding squeezing variance is given by $V^-_{\rm sq}(\delta\hat{Y}) = 0.74 \pm 0.02$. The anti–correlation signal $V(\delta\hat{Y}_a + \delta\hat{Y}_b)$ is 6dB above the noise level of the individual beams (trace 4). From the measured values, we can conclude that the examined state is non–separable, as can be seen when the measured values for the squeezing variances are plugged into eqn. (9):

$$V^+_{\rm sq}(\delta\hat{X}) + V^-_{\rm sq}(\delta\hat{Y}) = 0.55 + 0.74 = 1.29 \pm 0.03 < 2. \quad (14)$$

The asymmetry between the correlation measurements of the amplitude and the phase quadrature has basically two reasons: (i) Due to the finite interference contrast, as a result of imperfect mode matching [39] in the phase measuring setup, these measurements are less efficient than amplitude measurements, where no additional interference is required. Finite interference contrast characterized by the visibility $\mathcal{V} < 1$ has the effect of introducing additional losses. The loss is related to the visibility via $\mathcal{V}^2 = \eta$, where $\sqrt{1-\eta}$ is the corresponding signal at-

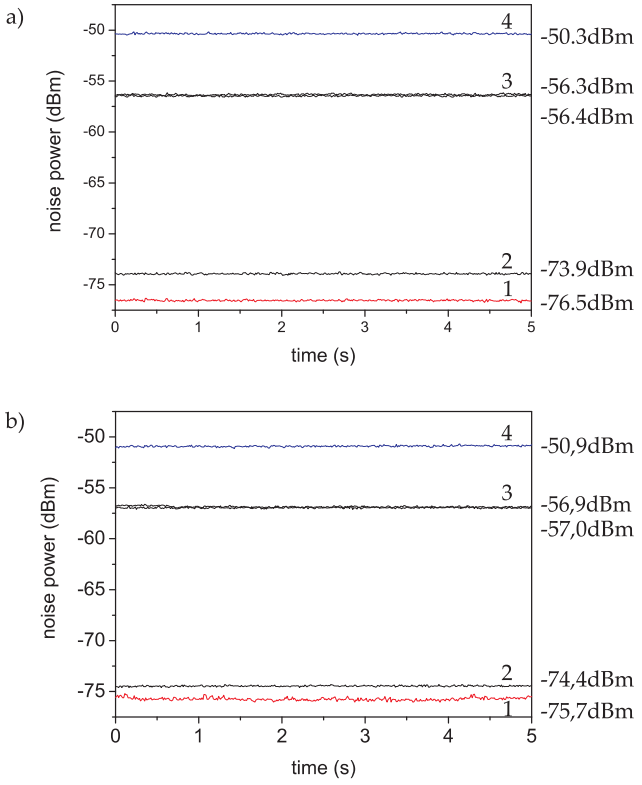

FIG. 4: Correlations of the (a) amplitude quadrature and (b) phase quadrature of the entangled beam pair measured with the unbalanced Mach–Zehnder interferometer. In each graph the noise level (traces 1) of the correlation signal is shown together with the corresponding shot-noise level (traces 2), the noise level of the individual beams (traces 3), and the signal with the anticorrelations (traces 4). The traces were corrected by subtracting the electronic noise, which was at −84.4 dBm. The measurement frequency was 20.5MHz. Similar results were presented in Ref. [20], however, the results shown here were obtained in a setup with improved performance.

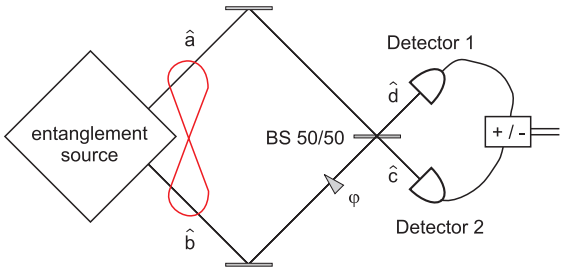

FIG. 5: Schematic setup for correlation measurements by interference of the entangled beam pair at a 50/50 beam splitter and direct detection

tenuation of the injected mode. (ii) As discussed in the previous section, due to slight asymmetries in the beam splitter for the entanglement generation, the phase correlations are degraded in the presence of a high degree of excess noise.

The major drawbacks of such an interferometer are its relative high losses due to the long propagation distances through several optical elements and finite mode matching quality: 10% losses are acquired during the propagation through the interferometer (back–reflection at lenses, losses at mirrors etc.), a visibility of $\mathcal{V} = 0.95$ is observed, corresponding to 10% loss, and the finite quantum efficiency of the photodiodes lead approximately to another 10% loss. The efficiency for phase quadrature measurements is therefore roughly 73%. In addition, when phase correlations on a pair of entangled beams are to be detected, four detectors are involved, each of which detects very noisy signals. Due to non–optimum balancing of the detection electronics, a slightly reduced correlation signal is obtained. Nevertheless, this apparatus is a very useful tool to directly measure the phase quadrature on intense light beams. The measurements above show that sub shot noise measurements of the phase quadrature are possible using this interferometer, thus making it a versatile apparatus for experiments in quantum optics. As an example, the phase measuring setup was applied in an experimental demonstration of continuous variable quantum erasing [40].

B. Interferometric determination of quadrature correlations

An alternative approach to construct the quadrature combinations that verify the correlations between potentially entangled beams is to interfere the entangled beam pair $\hat{a}_{\rm ent}$ and $\hat{b}_{\rm ent}$ at another 50:50 beam splitter as depicted in figure 5. Measurements of the quantum variables are not performed on the entangled beam pair individually, rather the joint quantum state of the beam pair is determined [25]. One advantage of this interferometric scheme is that information about the correlations in the phase quadrature can be obtained in direct detection without additional local oscillators or other phase measuring devices, making the experimental implementation easy. Furthermore, the cancellation of the correlated noise is done optically thus the requirements on the detectors are less stringent than in the previous case. Another advantage is that, entanglement can in principle be tested in a single measurement run contrary to the scheme in section IV.A where two successive measurements on the amplitude and phase quadrature must be performed.

To describe this interferometric technique, we consider the interference of the entangled beams with relative optical phase φ at a 50/50 beam splitter. The output modes after the interference are given by

$$\hat{c} = \frac{1}{\sqrt{2}}[\hat{a}_{\rm ent} - {\rm e}^{i\varphi}\hat{b}_{\rm ent}] \quad (15)$$

$$\hat{d} = \frac{1}{\sqrt{2}}[\hat{a}_{\rm ent} + {\rm e}^{i\varphi}\hat{b}_{\rm ent}]. \quad (16)$$

In both output ports of the interferometer, direct detection of the photon number is performed. The photon numbers are given by $\hat{n}_c = \hat{c}^\dagger\hat{c}$ and $\hat{n}_d = \hat{d}^\dagger\hat{d}$. The sum and the difference of the fluctuating parts of the photo currents immediately deliver the correlation signal for the amplitude and the phase quadrature of the entangled beams. For the moment, we are interested in an interference phase of $\varphi = \pi/2$, corresponding to equal intensity in the two output ports of the interferometer. The correlation signals are then given by a linear combination of the quadrature fluctuations of the entangled beam pair

$$\delta\hat{n}_c + \delta\hat{n}_d = \alpha_{\rm ent}\delta\hat{X}_{\rm a,ent} + \beta_{\rm ent}\delta\hat{X}_{\rm b,ent} \quad (17)$$

$$\delta\hat{n}_c - \delta\hat{n}_d = \beta_{\rm ent}\delta\hat{Y}_{\rm a,ent} - \alpha_{\rm ent}\delta\hat{Y}_{\rm b,ent}. \quad (18)$$

Depending on the classical amplitudes of the entangled beam pair, the detected correlation signal is scaled by the factors $\alpha_{\rm ent}$ and $\beta_{\rm ent}$.

As discussed in section II, the entangled beam pair is generated by the interference of squeezed beams of equal intensity α and relative optical phase θ. The amplitudes of the entangled field modes $\hat{a}_{\rm ent}$ and $\hat{b}_{\rm ent}$ are given by $\alpha\sqrt{1+\cos\theta}$ and $\alpha\sqrt{1-\cos\theta}$. Recall that maximal entanglement is generated, when the interference phase θ is such that the modes $\hat{a}$ and $\hat{b}$ have equal intensity ($\theta = \pi/2$). In that case, the non–separability properties of the two mode state can be checked directly in terms of the criterion by Duan and Simon [18, 19] given in eqn. (9). The respective values for the correlations in the amplitude and the phase quadrature, that is the squeezing variances $V^+_{\rm sq}(\hat{X})$ and $V^-_{\rm sq}(\hat{Y})$ could be found directly using equations (17) and (18) as $\alpha = \beta$. However, when the two potentially entangled beams have different classical amplitudes, as in the case when the interference phase to generate entanglement is non optimum $\theta \neq \pi/2$, non–symmetric linear combinations of the quadrature components are measured according to equations (17) and (18). Having such a linear combination at hand, a gener-

alized version of the non–separability criterion is needed as stated in [26, 41].

We define the operators $\delta\hat{u}$ and $\delta\hat{v}$, which are linear combinations of the quadrature operators $\delta\hat{X}_a$ and $\delta\hat{X}_b$ and $\delta\hat{Y}_a$ and $\delta\hat{Y}_b$

$$\delta\hat{u} = h_a\delta\hat{X}_a + h_b\delta\hat{X}_b \quad (19)$$

$$\delta\hat{v} = g_a\delta\hat{Y}_a + g_b\delta\hat{Y}_b. \quad (20)$$

Note that these new operators describe a two mode state, and the standard canonical commutation relations for single mode bosonic systems are no longer valid. However, these operators can be used to derive measureable quantities (bounderies) on non–separability as an extension to the criterion described by eqn. (9). A generalized criterion for non–separability then reads according to references [26, 41]

$$\langle(\Delta\hat{u})^2\rangle + \langle(\Delta\hat{v})^2\rangle \leq 2(|h_a g_a| + |h_b g_b|). \quad (21)$$

For the case described above, we easily find that $g_a = h_b = \alpha\sqrt{1+\cos\theta}$ and $h_a = -g_b = \alpha\sqrt{1-\cos\theta}$ by comparing (17) and (18) with (19) and (19). Using these relations and normalizing to the quantum noise limit, the criterion for non–separability adapted to our experimental configuration can be written as

$$\langle(\Delta\hat{u})^2\rangle_{\rm norm} + \langle(\Delta\hat{v})^2\rangle_{\rm norm} \leq 2\sqrt{1-\cos^2\theta}. \quad (22)$$

From this equation it is evident that for finite values of initial squeezing and for interference phases $\theta \neq \pi/2$ it becomes harder to show that the given beam pair is entangled as the right hand side of the inequality is getting smaller. Using that criterion, only for infinite input squeezing, entanglement is revealed for any phase $\theta \neq 0$. As long as $\theta \neq 0$, entanglement is always generated with our scheme, although it will not be witnessed by that criterion.

Interestingly, the parameters g and h can always be optimized such that one can observe always as much correlations below the quantum noise limit as there is initial squeezing. For the entangled states given in eqns. (3)–(6), these optimized gain factors to recover the full correlation signal coincide with the amplitudes $\alpha_{\rm ent}$ and $\beta_{\rm ent}$ as given in eqns. (1) and (2). The left hand side of inequality (22) can thus be optimized to yield the same value independent of θ corresponding to the initial squeezing level. From comparison with eqns. (17) and (18) we see that by using the interferometric measurement apparatus, optimized correlation signals are measured automatically, provided the second interference phase is chosen such that the two output modes $\hat{c}$ and $\hat{d}$ have the same intensity. However, we point out that these correlations do not imply maximum possible entanglement, as the boundary on the right hand side of (22) has to be adjusted and the degree of violation of the unequality changes with θ.

Let us for the moment consider the case $\theta = \pi/2$, so maximum possible entanglement is generated. Using the strategy described above, the correlations in the amplitude and the phase quadrature are detected experimentally. The two entangled beams interfere at a 50/50 beam splitter, the noise variance of the sum– and the difference signal of the photo currents are recorded. The measurement technique used here is closely related to the one used for dense coding by Li et al. [42]. The results of such measurements are shown in figure 6. In (a) the noise variance of the sum signal, that is the correlation signal $V(\delta\hat{X}_a + \delta\hat{X}_b)$ of the amplitude quadrature is plotted together with the shot noise level. The correlation signal is 3.3dB below the quantum noise limit, corresponding to a squeezing variance of $V^+_{\rm sq}(\delta\hat{X}) = 0.47 \pm 0.02$. The correlation signal for the phase quadrature follows from the difference signal of the photo current and is plotted in (b). The correlations $V(\delta\hat{Y}_a - \delta\hat{Y}_b)$ of the phase quadrature are 2.1dB below the quantum noise limit, the squeezing variance is $V^-_{\rm sq}(\delta\hat{Y}) = 0.62 \pm 0.02$. From the sum of the squeezing variances

$$V^+_{\rm sq}(\delta\hat{X}) + V^-_{\rm sq}(\delta\hat{Y}) = 0.47 + 0.62 = 1.09 \pm 0.03 < 2 \quad (23)$$

we can conclude the non–separability of the two mode state. Again, the asymmetry between the sum and the

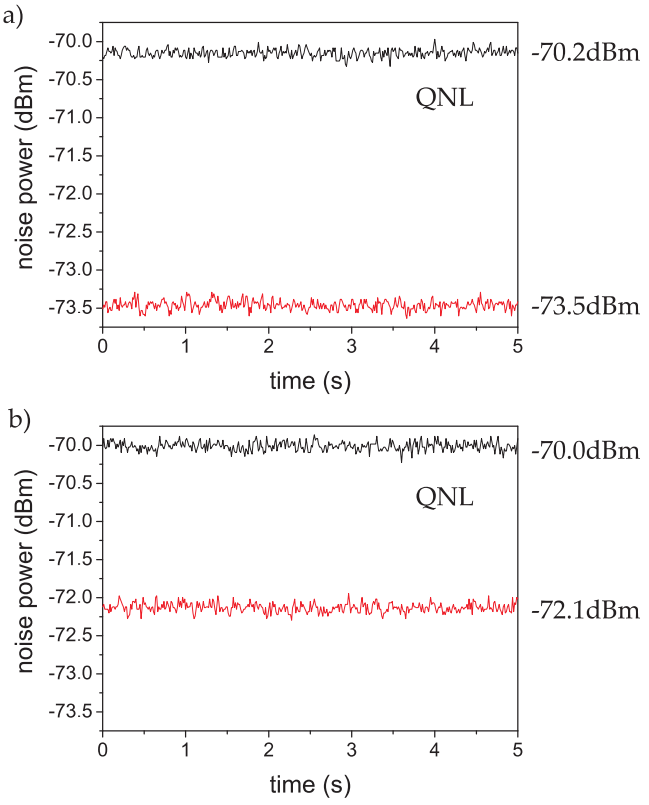

FIG. 6: Correlations of the (a) amplitude quadrature and (b) phase quadrature of the entangled beam pair measured via interference and direct detection. In the graph the noise level of the correlation signal is shown together with the corresponding shot-noise level. The traces were corrected by subtracting the electronic noise, which was at −87.8 dBm. The measurement frequency was 17.5MHz.

difference channel, i. e. the correlations in the amplitude– and the phase quadrature is due to the slightly unbalanced beam splitting ratio in the entanglement generation scheme and in the interferometric verification scheme together with the high degree of excess noise of the initial squeezed states. The input squeezing used for the entanglement generation in this and in the following experiment was also characterized with the given set up. We measured 3.7 ± 0.2dB (3.8 ± 0.2dB) for the p (s)–polarized input fields. When compared to the measurement scheme where two independent phase measuring devices are used(Section IV.A), this setup is more efficient and, as expected, the detected correlations and squeezing levels are larger.

C. Direct experimental test of non–separability

The third measurement scheme is a variation of the interferometric scheme shown in figure 5. In contrast to the previous measurement strategy, detection is performed in one output port only. For a particular choice of the relative phase φ, a signal is obtained that can be directly used to check non–separability as stated in eqn. (9). Direct detection of the noise variances for the photon numbers of the output modes $\hat{c}$ or $\hat{d}$ deliver the desired correlation signal[24]:

$$\begin{aligned} V(\delta\hat{n}_{c,d}) &= \frac{1}{2}\alpha^2(1 \pm \cos\varphi)^2 V_{\rm sq}^{+}(\delta\hat{X}) \\ &+ \frac{1}{2}\alpha^2 \sin^2\varphi V_{\rm sq}^{-}(\delta\hat{Y}). \end{aligned} \tag{24}$$

The corresponding quantum noise limits are

$$V(\delta\hat{n}_{c,d,coh}) = \alpha^2(1 \pm \cos\varphi). \tag{25}$$

Normalizing (24) to the quantum noise limit, one obtains

$$\begin{aligned} & V(\delta\hat{X}_{c,d})_{\rm norm} \\ &= \frac{1}{2}\left[(1 \pm \cos\varphi)V_{\rm sq}^{+}(\delta\hat{X}) + \frac{\sin^2\varphi}{(1 \pm \cos\varphi)} V_{\rm sq}^{-}(\delta\hat{Y})\right] \end{aligned} \tag{26}$$

For the interference phase $\varphi = \pi/2$ the detected signal in one output mode reduces to

$$V(\delta\hat{X}_{c,d})_{\rm norm} = \frac{1}{2}\left[V_{\rm sq}^{+}(\delta\hat{X}) + V_{\rm sq}^{-}(\delta\hat{Y})\right] \tag{27}$$

which is exactly the measure one needs to prove non–separability according to the Duan–Simon criterion. The two–mode state is therefore entangled, if noise reduction in the output ports $\hat{c}$ or $\hat{d}$ are observed.

The results of such measurements on modes $\hat{c}$ and $\hat{d}$ are plotted in figure 7. The recorded noise level of the modes is plotted together with the shot noise level. Both output modes are squeezed, and we measure $V(\delta\hat{X}_c)_{\rm norm} = 0.52 \pm 0.02$ (see figure 7 (a)) and $V(\delta\hat{X}_d)_{\rm norm} = 0.55 \pm 0.02$

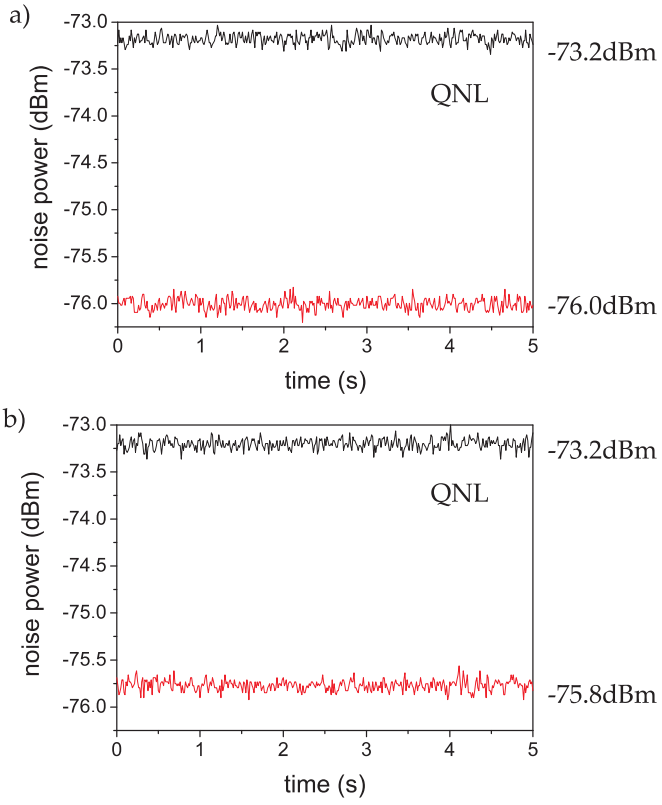

FIG. 7: Direct detection of non–separability. Both entangled beams were brought to interference, the noise power is measured in the individual output ports. Amplitude squeezing of 2.8dB and 2.6dB below the shot noise level is observed. the measurement frequency was 17.5MHz, the electronic noise level was at -87.8dBm.

(see 7 (b)). From these noise levels we obtain the sum of the squeezing variances

$$V_{\rm sq}^{+}(\delta\hat{X}) + V_{\rm sq}^{-}(\delta\hat{Y}) = 1.05 \pm 0.04 < 2, \tag{28}$$

$$V_{\rm sq}^{+}(\delta\hat{X}) + V_{\rm sq}^{-}(\delta\hat{Y}) = 1.10 \pm 0.04 < 2, \tag{29}$$

for the measurements in the output ports $\hat{c}$ and $\hat{d}$, respectively. The values are in good agreement with the measurement results of the previous section, where the correlations of the amplitude and the phase quadrature have been determined separately by using the sum– and the difference channel of both output ports $\hat{c}$ and $\hat{d}$. The results shown in Fig. 7 were obtained by an improved version of the measurement reported by Silberhorn et al. [16]. In contrast to earlier measurements, the two phases θ and φ are now stabilized and, most importantly, the phase θ was adjusted to $\pi/2$ so that the non–separability criterion holds in its standard form (see eqns. (9) and (22)).

To conclude from such measurements that the beam pair under investigation is indeed entangled when noise reduction in the output modes is observed, requires that both beams have equal intensity. Then the Duan–Simon criterion in the form (9) can be applied directly to check

for non–separability. Note that in this case squeezing is observed in the two output ports of the interference for any value of φ as can be seen from equation (26). For all other values of θ, i. e. $\theta \neq \pi/2$, more general criteria have to be applied to check for entanglement, like those given in equation (21). In this situation however, the expression (26) to describe the noise power in one output port of the interferometer as a function of the interference phase φ looks more complicated.

We summarize and compare the results of the different methods to characterize entanglement of intense light beams in Table I. All methods deliver roughly the same

	Method	$V_{\rm sq}^{+}(\delta\hat{X}) + V_{\rm sq}^{-}(\delta\hat{Y})$
A.	Phase measuring interferometer	1.29 ± 0.03
B.	Measure correlations interferometrically	1.09 ± 0.03
C.	Direct test of non–separability	1.05 ± 0.04 (output $\hat{c}$) 1.10 ± 0.04 (output $\hat{d}$)

TABLE I: Comparison of the different methods to verify entanglement of intense, pulsed light. For each method, the experimental results for the inseparability criterion $V_{\rm sq}^{+}(\delta\hat{X}) + V_{\rm sq}^{-}(\delta\hat{Y}) < 2$ as stated in eqn. (9) are noted.

results, and we note in particular that their estimated errors are of the same order. However, method A cannot be compared directly with the other two methods (B and C) since the measurement frequency was 20.5MHz in the former case while it was 17.5MHz in the latter case. The slightly poorer results of method A can be explained easily by its higher intrinsic losses that reduce the degree of quantum correlations. Depending on the type of applications and whether or not it is possible to bring the entangled beams to interference, one can choose the most appropriate way to access information about the quantum correlations of a beam pair.

V. CONCLUSIONS

In this paper, we have presented a comprehensive study of a fiber optical entanglement source with bright, pulsed light. The source is rather compact, robust and easy to handle. Not only entanglement generation was shown, but also different measurement tools were provided to detect entanglement. Hence these methods can be readily implemented in protocols for quantum communication and quantum information processing. These schemes all rely on interference effects, thus they are suited to handle intense beams as they do not require external local oscillators. Stable operation and the generation of correlations well beyond the quantum noise limit was demonstrated. For a certain class of applications, such as entanglement swapping or quantum dense coding with continuous variables, the high degree of excess noise introduced in the fibers, limits the efficiency and performance of these protocols. However, the problem of excess noise might be overcome by using microstructured fibers for the squeezing generation. New experiments indicate that less thermal noise is generated when these fibers are used instead of standard fibers [43]. Less thermal noise would also improve the measurement accuracy, as the required dynamic range to be handled in the detection electronics could be considerably reduced. Together with general improvements in the detection electronics this gives potential for improved entanglement generation and detection using the fiber setup. The whole setup could be simplified further by changing to a fiber integrated Sagnac loop for the squeezed state generation, as was demonstrated in reference [44].

Acknowledgments

We want to acknowledge helpful discussions with P. van Loock. This work was supported by the Schwerpunktprogramm 1078 of the Deutsche Forschungsgemeinschaft (QIV), the Kompetenznetzwerk Quanteninformationsverarbeitung of the state of Bavaria (A8) and the EU project COVAQIAL (project no. FP6-511004).

[1] A. Einstein, B. Podolsky, and N. Rosen, Physical Review **47**, 777 (1935).
[2] M. A. Nielsen and I. L. Chuang, *Quantum Computation and Quantum Information* (Cambridge University Press, Cambridge, 2000).
[3] C. H. Bennett, G. Brassard, C. Crepeau, R. Jozsa, A. Peres, and W. K. Wootters, Physical Review Letters **70**, 1895 (1993).
[4] C. H. Bennett and S. J. Wiesner, Physical Review Letters **69**, 2881 (1992).
[5] S. L. Braunstein and A. K. Pati, eds., *Quantum Information with Continuous Variables* (Kluwer Akademic Press, Dordrecht, 2003).
[6] Z. Y. Ou, S. F. Pereira, H. J. Kimble, and K. C. Peng, Physical Review Letters **68**, 3663 (1992).
[7] Y. Zhang, H. Wang, X. Li, J. Jing, C. Xie, and K. Peng, Physical Review A **62**, 023813 (2000).
[8] J. Laurat, T. Coudreau, G. Keller, N. Treps, and C. Fabre, Phys. Rev. A **70**, 042315 (2004).
[9] C. Schori, J. L. Sørensen, and E. S. Polzik, Physical Re-

view A **66**, 033802 (2002).
[10] A. S. Villar, L. S. Cruz, K. N. Cassemiro, M. Martinelli, and P. Nussenzveig, arXiv:quant–ph/0506139 (2002).
[11] J. Wenger, A. Ourjoumtsev, R. Tualle-Brouri, and F. Grangier, Eur. Phys. J. D **32**, 391 (2004).
[12] A. Furusawa, J. Sørensen, S. Braunstein, C. Fuchs, H. Kimble, and E. Polzik, Science **282**, 706 (1998).
[13] W. P. Bowen, R. Schnabel, P. K. Lam, and T. C. Ralph, Physical Review Letters **90**, 043601 (2003).
[14] T. Aoki, N. Takei, H. Yonezawa, K. Wakui, T. Hiraoka, A. Furusawa, and P. van Loock, Physical Review Letters **91**, 080404 (2003).
[15] V. Josse, A. Dantan, A. Bramati, M. Pinard, and E. Giacobino, Physical Review Letters **92**, 123601 (2004).
[16] C. Silberhorn, P. K. Lam, O. Weiß, F. König, N. Korolkova, and G. Leuchs, Physical Review Letters **86**, 4267 (2001).
[17] M. D. Reid and P. D. Drummond, Physical Review Letters **60**, 2731 (1988).
[18] L. M. Duan, G. Giedke, J. I. Cirac, and P. Zoller, Physical Review Letters **84**, 2722 (2000).
[19] R. Simon, Physical Review Letters **84**, 2726 (2000).
[20] O. Glöckl, U. L. Andersen, S. Lorenz, C. Silberhorn, N. Korolkova, and G. Leuchs, Optics Letters **29**, 1936 (2004).
[21] T. C. Ralph and P. K. Lam, Physical Review Letters **81**, 5668 (1998).
[22] G. Leuchs, T. Ralph, C. Silberhorn, and N. Korolkova, Journal of Modern Optics **46**, 1927 (1999).
[23] M. S. Kim, W. Son, V. Buzek, and P. L. Knight, Phys. Rev. A **65**, 032323 (2002).
[24] N. Korolkova, C. Silberhorn, O. Glöckl, S. Lorenz, C. Marquardt, and G. Leuchs, European Physical Journal D **18**, 229 (2002).
[25] S. M. Tan, Physical Review A **60**, 2752 (1999).
[26] V. Giovannetti, S. Mancini, D. Vitali, and P. Tombesi, Physical Review A **67** 022320(2003).
[27] P. Hyllus, and J. Eisert, arXiv:quant–ph/0510077 (2005).
[28] S. Schmitt, J. Ficker, M. Wolff, F. König, A. Sizmann, and G. Leuchs, Physical Review Letters **81**, 2446 (1998).
[29] D. Krylov and K. Bergman, Optics Letters **23**, 1390 (1998).
[30] M. Fiorentino, J. E. Sharping, P. Kumar, D. Levandovsky, and M. Vasilyev, Physical Review A **64**, 031801(R) (2001).
[31] J. Heersink, T. Gaber, S. Lorenz, O. Glöckl, N. Korolkova, and G. Leuchs, Phys. Rev. A **68**, 013815 (2003).
[32] R. M. Shelby, P. D. Drummond, and S. J. Carter, Physical Review A **42**, 2966 (1990).
[33] R. M. Shelby, M. D. Levenson, and P. W. Bayer, Physical Review Letters **54**, 939 (1985).
[34] H. P. Yuen and V. Chan, Optics Letters **8**, 177 (1983).
[35] A. E. Siegman, *Lasers* (University Science Books, Mill Valley, 1986).
[36] P. Galatola, L. A. Lugiato, P. M. G., P. Tombesi, and G. Leuchs, Optics Communications **85**, 95 (1991).
[37] R. M. Shelby, M. D. Levenson, S. H. Perlmutter, R. G. DeVoe, and D. F. Walls, Phys. Rev. Lett. **57**, 691 (1986).
[38] H. A. Bachor, M. D. Levenson, D. F. Walls, S. H. Perlmutter, and R. M. Shelby, Phys. Rev. A **38**, 180 (1988).
[39] J. Gea-Banacloche and G. Leuchs, Journal of Modern Optics **36**, 1277 (1989).
[40] U. L. Andersen, O. Glöckl, S. Lorenz, G. Leuchs, and R. Filip, Phys. Rev. Lett. **93**, 100403 (2004).
[41] S. L. Braunstein and P. van Loock, Rev. Mod. Phys. **77**, 513 (2005).
[42] X. Li, Q. Pan, J. Jing, J. Zhang, C. Xie, and K. Peng, Physical Review Letters **88**, 047904 (2002).
[43] A. Korn, O. Glöckl, S. Lorenz, C. Marquardt, U. L. Andersen, and G. Leuchs, CLEO/IQEC and PhAST Technical Digest on CDROM (The Optical Society of America, Washington, DC, 2004), ITuI37.
[44] M. Meißner, C. Marquardt, J. Heersink, T. Gaber, A. Wietfeld, G. Leuchs, and U. L. Andersen, J. Opt. B: Quantum Semiclass. Opt. **6**, S652 (2004).